

See discussions, stats, and author profiles for this publication at: <https://www.researchgate.net/publication/278397945>

Laser Emission from Ring Resonators Formed by a Quantum-Dot-Doped Single Polymer Nanowire

ARTICLE in ACS MACRO LETTERS · DECEMBER 2014

Impact Factor: 5.76 · DOI: 10.1021/mz500663t

READS

50

2 AUTHORS:



Xianguang Yang

Sun Yat-Sen University

5 PUBLICATIONS 10 CITATIONS

SEE PROFILE



Baojun Li

Sun Yat-Sen University

159 PUBLICATIONS 1,459 CITATIONS

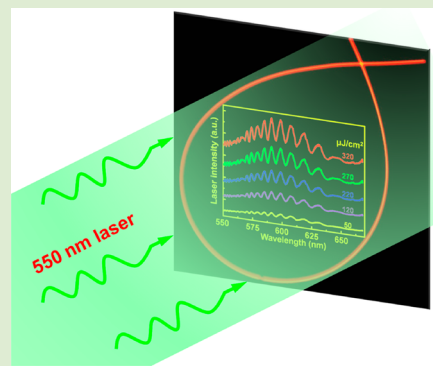
SEE PROFILE

Laser Emission from Ring Resonators Formed by a Quantum-Dot-Doped Single Polymer Nanowire

Xianguang Yang and Baojun Li*

State Key Laboratory of Optoelectronic Materials and Technologies, School of Physics and Engineering, Sun Yat-Sen University, Guangzhou 510275, China

ABSTRACT: Laser emission from nanowire-based devices is important for nanophotonic applications. Here we report the observation of optically pumped laser emission from ring resonators formed by quantum-dot-doped single polymer nanowire. By assembling a 500 nm diameter single polymer nanowire with an optical loss coefficient of 70 cm^{-1} to form a ring resonator with a short diameter of $20\text{ }\mu\text{m}$ and a large diameter of $40\text{ }\mu\text{m}$, multimode laser emission with mode number of 9 is obtained in the wavelength region from 550 to 650 nm. The dominant emission is 600 nm wavelength with a line width of 0.8 nm, a Q factor of 400, and a low lasing threshold of $100\text{ }\mu\text{J}/\text{cm}^2$ under a 550 nm green laser pump.



Owing to their excellent ability to emit, transmit, and modulate light in various architectures, organic nanomaterials have been attracting great interest in constructing nanoscale photonic devices and circuits.^{1–3} Optical properties of one-dimensional organic nanomaterials are fundamentally different from those of inorganic counterparts,^{4,5} particularly in quantum-dot-doped polymer nanowires. Because of high photoluminescence efficiency and large stimulated emission cross sections ($\sim 10^{-15}\text{ cm}^2$), polymer nanowires can enhance the performance of nanophotonic devices.^{6–8} Recently, considerable progress has been achieved in developing subwavelength sized optically pumped lasers in polymer nanowires, which can be used for assembly and manipulation of arbitrary structures.^{9–13} The optical pumping of those nanowires exhibits attractive qualities such as narrow line width, high Q factor, and low threshold, which are promising for their application in bioimaging and optical sensing.^{14–16} In a variety of subwavelength sized optically pumped lasing structures, the knot resonator,¹⁷ microring,¹⁸ and loop resonator¹⁹ are more attractive because resonance occurs when the optical path of the resonator is equal to an integer multiple of the resonance wavelengths, which support multiple resonances.²⁰ These ring resonators show interesting emission efficiency and laser action. However, the lasing threshold is up to $2.6\text{ mJ}/\text{cm}^2$.¹⁷ In this work, we report a ring resonator-based multimode laser emission with low lasing threshold of $100\text{ }\mu\text{J}/\text{cm}^2$, which is formed by CdSe–ZnS core–shell quantum dot (QD) doped polyvinylpyrrolidone (PVP) single nanowires. The reason why we chose PVP and QDs is that PVP is an amphiphilic surfactant which can render the nanocrystals dispersible in water,²¹ while QDs are a promising gain media for lasing.²² Interestingly, the influence of ring resonator size and shape on Q factor, mode number, and spectrum has been demonstrated.

QDs and PVP ($n = 1.48$) were purchased from Zkwy Bio-Tech and Boai NKY companies, respectively. The QD-doped polymer nanowires were fabricated by a direct drawing method as follows: First, 680 mg of PVP was dissolved in 0.8 mL of anhydrous ethanol to form homogeneous PVP ethanol solution. Second, 340 μL of QD (5 nm in diameter) aqueous solution (concentration 4 $\mu\text{M}/\text{L}$) was diluted in the PVP ethanol solution. The mixture was stirred at room temperature for 3 h and followed by a 40 min ultrasound to form a uniform solution with an appropriate viscosity for drawing. Third, the tip of a tapered silica fiber (diameter $\sim 125\text{ }\mu\text{m}$) was immersed into the mixture solution for 1–3 s and then pulled out with a speed of 0.1–2 m/s, leaving a QD-doped polymer wire extending between the solution and the fiber tip with very fast evaporation of the ethanol. The diameter of the polymer wires varies from 300 to 900 nm.

Figure 1a shows a typical scanning electron microscope (SEM, HIROX, SH-5000M) image of a coiled single polymer nanowire (average diameter $\sim 500\text{ nm}$, length $\sim 1.25\text{ mm}$) containing QDs. Figure 1b shows the SEM image of nanowires 1–4 with diameters of about 900, 400, 400, and 500 nm, respectively. Nanowires 1 and 2 are in parallel, while nanowires 3 and 4 are crossed. Figure 1c shows a high-resolution SEM image of a 300 nm diameter nanowire. To closely inspect the QD distribution in the nanowire, energy-dispersive X-ray spectroscopy (EDS) and transmission electron microscopy (TEM) (operated at 300 kV) were performed and shown in Figure 1d. It can be seen from the inset TEM image that the QDs (as indicated by yellow arrows) were successfully doped in

Received: October 17, 2014

Accepted: December 3, 2014

Published: December 4, 2014



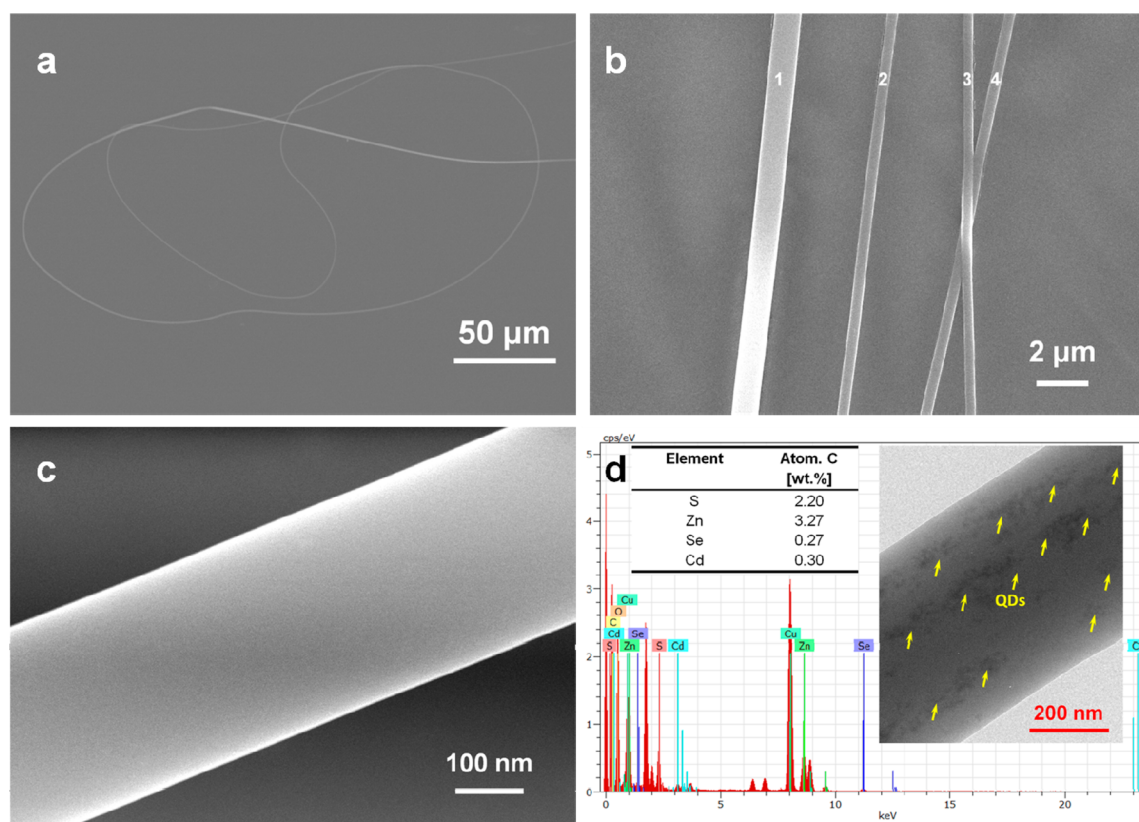


Figure 1. SEM and TEM images of QD-doped polymer nanowires and EDS analysis. (a) SEM image of a coiled QD-doped polymer nanowire. (b) SEM image of nanowires 1–4 with diameters of about 900, 400, 400, and 500 nm, respectively. (c) High-resolution SEM image of a 300 nm diameter nanowire. (d) EDS spectrum and TEM image of a 500 nm diameter nanowire. The yellow arrows indicate the doped QDs.

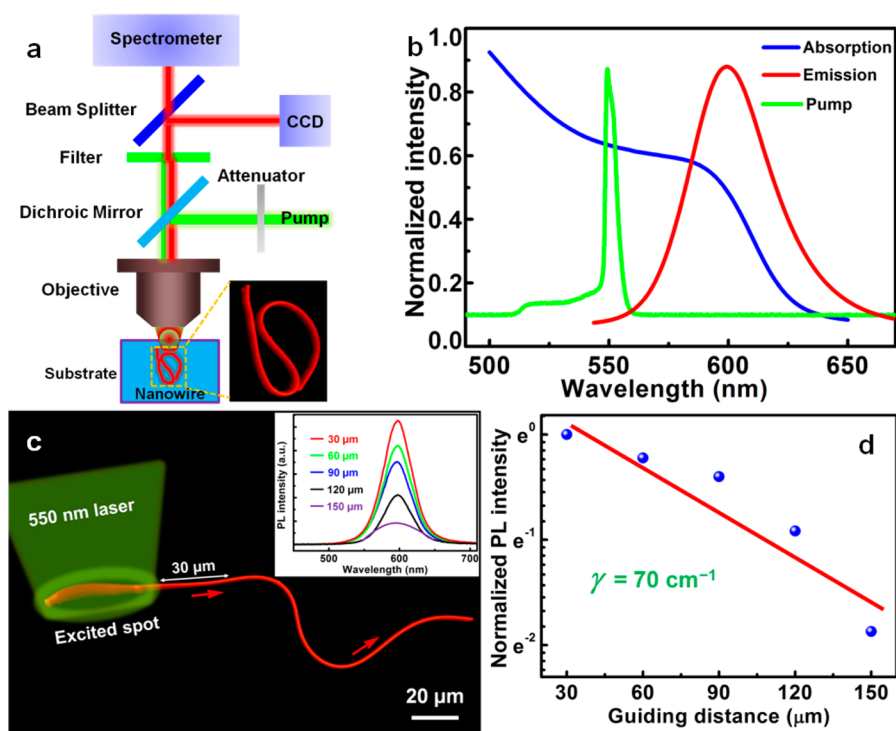


Figure 2. (a) Schematic experimental setup. (b) Normalized spectra of absorption, emission, and pump laser. (c) A dark-field PL microscope image of a QD-doped polymer nanowire with a diameter of 500 nm and a length of 200 μm , which is locally excited at one end with an optical pump of 100 $\mu\text{J}/\text{cm}^2$. The red arrows show the guiding direction of light. Inset: measured PL spectra at different positions along the nanowire. (d) Normalized PL intensity versus guiding distance along the nanowire.

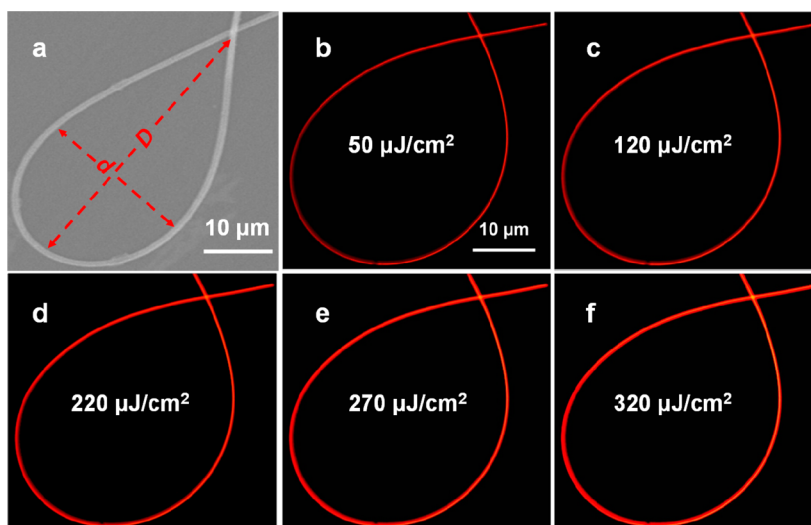


Figure 3. (a) SEM image of a ring resonator formed by a 500 nm diameter QD-doped polymer nanowire with $D = 40 \mu\text{m}$ and $d = 20 \mu\text{m}$. (b–f) Dark-field PL microscope images at different optical pumps. Scale bar in panel b is applicable to panels c–f.

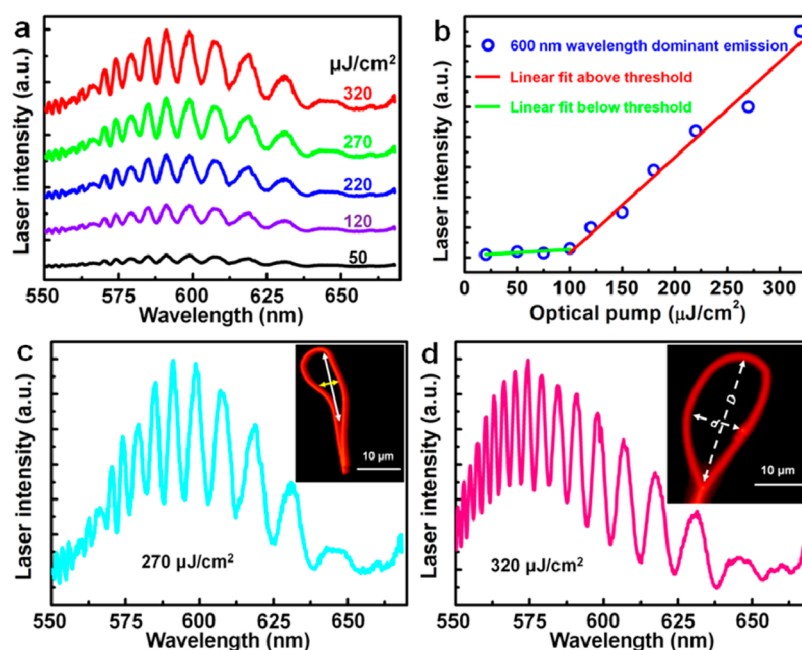


Figure 4. (a) Nanowire laser emission spectra for different incident optical pumps. (b) Laser emission intensity at 600 nm wavelength versus optical pump, indicating a lasing threshold of about $100 \mu\text{J}/\text{cm}^2$. (c) Multimode laser emission spectrum of a ring resonator at an optical pump of $270 \mu\text{J}/\text{cm}^2$. Inset: dark-field PL image of the ring resonator with circumference of $60 \mu\text{m}$ formed by a 500 nm diameter polymer nanowire. The large diameter of the ring is $16 \mu\text{m}$ (as indicated in white double arrow line), while the short diameter is $5 \mu\text{m}$ (as indicated in yellow double arrow line). (d) Multimode laser emission spectrum of a ring resonator at an optical pump of $320 \mu\text{J}/\text{cm}^2$. Inset: dark-field PL image of the ring resonator with circumference of $70 \mu\text{m}$ formed by a 500 nm diameter polymer nanowire with $D = 26 \mu\text{m}$ and $d = 11 \mu\text{m}$.

the 500 nm diameter nanowire with estimated maximum diameter variation $\Delta D \approx 15 \text{ nm}$ over a length $L = 700 \text{ nm}$. The EDS analysis confirms the existence of S (2.20 wt %), Zn (3.27 wt %), Se (0.27 wt %), and Cd (0.30 wt %) elements. The estimated concentration of the doped QDs is $3.5 \times 10^3 \mu\text{m}^{-3}$.

Optical characterization of the polymer nanowires was carried out under an optical microscope using an experimental setup as schematically shown in Figure 2a. A 550 nm picoseconds pulsed laser (10 kHz repetition rate, 300 ps pulse width) was used to pump the nanowires. The pump laser was focused to a spot with a size of $\sim 50 \mu\text{m}$ through a $100\times$ objective (numerical aperture $\text{NA} = 0.65$). The photo-

luminescence (PL) signals were collected by the same objective and directed through a dichroic mirror and a 550 nm notch filter. The filtered light was split by a beam splitter and directed to a spectrometer and a CCD camera for spectrum and image measurement, respectively. Figure 2b shows normalized spectra of the 550 nm pump laser, absorption, and emission. The emission spectrum is centered at 600 nm with a full width at half-maximum of about 41 nm which is the gain spectrum profile for laser emission. Waveguiding properties of the QD-doped polymer nanowires were investigated by focusing the 550 nm laser on the distal end of the nanowire. PL signals were collected along the nanowire through a Micro spectrophoto-

tometer (CRAIC 20/20 PV). Figure 2c shows a dark-field PL microscope image of a QD-doped polymer nanowire with a diameter of 500 nm and a length of 200 μm , which is locally excited at one end with an optical pump of 100 $\mu\text{J}/\text{cm}^2$. The inset shows PL spectra collected at different guiding distances from the excited spot with a guiding distance interval of 30 μm . Figure 2d shows the relationship of normalized PL intensity as a function of guiding distance. The result indicates that the normalized PL intensity decreases exponentially with an increase of the guiding distance, which is a typical characteristic of active waveguides.¹¹ The PL intensity data are well-fitted by the equation $I = I_0 \exp(-\gamma d)$, where I is the measured PL intensity, I_0 a pre-exponential factor which indicates the PL intensity measured at very small d values, d the guiding distance, and $\gamma = 70 \text{ cm}^{-1}$ the optical loss coefficient. It is worth noting that the mechanisms affecting optical loss of the polymer nanowire are self-absorption, Rayleigh scattering, surface-mediated loss, evanescent coupling of light into the underlying substrate, and confinement effects.¹¹ Normally, self-absorption will lead to a red-shift in PL spectrum. From the inset of Figure 2c, no red-shift occurred because the doped QD concentration is $3.5 \times 10^3 \mu\text{m}^{-3}$ ($< 5.5 \times 10^3 \mu\text{m}^{-3}$), which is in accordance with previously reported work.^{15,23} Second, some light escapes laterally from the body of the polymer nanowire due to surface-assisted scattering. These losses involve light propagating at angles larger than the critical one (strictly related to the orientation of the QD emitting dipoles inside the nanowire), supported by surface roughness.²⁴ However, due to the absence of significant scattering spots along the nanowire body, this mechanism is a minor process contributing to the measured optical losses. Finally, three other mechanisms play a major role in this work. In addition, we can minimize evanescent coupling of light from the polymer nanowires into the surrounding media by suspending the polymer nanowires in air.

To investigate the lasing properties of ring resonator, a 500 nm diameter QD-doped polymer nanowire was micromanipulated into a ring resonator. Figure 3a shows its SEM image with the large ring diameter $D = 40 \mu\text{m}$ and the short ring diameter $d = 20 \mu\text{m}$. The resonator was entirely irradiated by the 550 nm laser beam through a 100 \times objective with a focused spot of about 50 μm . Figures 3b–f show dark-field PL microscope images of the ring resonator pumped by 50, 120, 220, 270, and 320 $\mu\text{J}/\text{cm}^2$, respectively. It should be pointed out that a little difference between the shapes of the SEM image and the dark-field PL microscope images is due to unavoidable vibration during the move from PL image to SEM image measurement.

The PL signals from the ring resonator were collected through an objective and measured by a spectrometer. Figure 4a shows laser emission spectra from the ring resonator at different incident optical pumps. Figure 4b shows the relationship between the integrated intensity of laser emission around the 600 nm wavelength and the optical pump, indicating a lasing threshold of about 100 $\mu\text{J}/\text{cm}^2$, which is 1 order of magnitude lower than that (2.6 mJ/cm^2) of the dye-doped polymer nanofiber knot resonator.¹⁷ With an increase in the optical pump, multiple resonance peaks appeared in the wavelength region from 550 to 650 nm (Figure 4a). According to the whispering gallery mode theory,^{25,26} the free spectral range is $\text{FSR} \approx \Delta\lambda = \lambda^2/2nL$, where λ is the resonant wavelength, L the circumference of the ring resonator, and n the refractive index of QD-doped PVP. Compared with pure PVP ($n = 1.48$, no QDs doped), the refractive index of QD-doped PVP is $n = 1.5$, which is estimated according to

previously reported work.^{27,28} Thus, the calculated $\text{FSR} \approx 1.2 \text{ nm}$ is close to the measured FSR in the spectrum of 1.5 nm (Figure 4a, optical pump of 320 $\mu\text{J}/\text{cm}^2$). The small difference can be attributed to the equation $\text{FSR} \approx \Delta\lambda = \lambda^2/2nL$ which is an approximation because the effect of the substrate dielectric on phase dispersion is neglected.²⁹ The resonator quality factor $Q = \lambda/\Delta\lambda$ was calculated to be 400 at 600 nm resonant wavelength.³⁰ The quality factor can be tuned via the proper control of ring resonator size. For example, Figure 4c shows the multimode laser emission spectrum of a ring resonator with mode number of 9 at an optical pump of 270 $\mu\text{J}/\text{cm}^2$. The inset shows the dark-field PL image of the ring resonator with circumference of 60 μm formed by a 500 nm diameter polymer nanowire. The calculated $\text{FSR} \approx 2 \text{ nm}$ is close to the measured FSR in the spectrum of 2.2 nm. Thus, the calculated Q factor is 273 at 600 nm resonant wavelength. For comparison, Figure 4d shows the multimode laser emission spectrum of a ring resonator with mode number of 8 at an optical pump of 320 $\mu\text{J}/\text{cm}^2$. The inset shows the dark-field PL image of the ring resonator with circumference of 70 μm formed by a 500 nm diameter polymer nanowire. The calculated $\text{FSR} \approx 1.7 \text{ nm}$ is close to the measured $\text{FSR} \sim 2 \text{ nm}$ in the spectrum. Thus, the calculated Q factor is 300 at 600 nm resonant wavelength. Note that the mode number is related to a balance between the FSR and PL gain spectrum profile of QDs. Additionally, from Figures 4c and 4d, it can be seen that the shape of the multimode laser emission spectrum is strongly dependent on the geometry of the ring resonator. This provides an opportunity for the tunable multimode emission spectrum via the proper design of the ring resonator. Overall, these results indicate that the Q factor, mode number, and multimode laser emission spectrum can be well controlled through careful micromanipulation of the polymer nanowire. Also, for individual resonance peaks in Figure 4d, the lasing wavelength of the dominant mode blue-shifts from 600 to 599 nm, as illustrated in Figures 4c and 4d with the incident optical pump of 270 and 320 $\mu\text{J}/\text{cm}^2$, respectively. This phenomenon manifests the frequency pulling effect in laser oscillations.^{31,32} From the above results, it can be seen that pulling effect, size, and shape of the ring resonator influence the spectral characteristics of the polymer nanowire ring resonator laser simultaneously. It is important to control them carefully for scientific research and practical applications. Although the multimode laser with low lasing threshold operated in the 550–650 nm spectral range has been demonstrated with a QD-doped single polymer nanowire, a wide wavelength tunable single-mode nanowire laser may be possible through the design of a self-coupled resonator for mode selection.²⁶

In conclusion, a ring resonator-based multimode laser structure was successfully fabricated with the micromanipulation of a QD-doped single polymer nanowire. The polymer nanowire with an optical loss coefficient of 70 cm^{-1} was assembled into a ring resonator with a short diameter of 20 μm and a large diameter of 40 μm . Under 550 nm green laser pumping, multimode laser emission with mode number of 9 in the wavelength region from 550 to 650 nm was obtained for the ring resonator. The dominant emission is at around 600 nm wavelength with a line width of 0.8 nm, a Q factor of 400, and a lasing threshold as low as 100 $\mu\text{J}/\text{cm}^2$. In addition, the influence of ring resonator size and shape on Q factor, mode number, and spectrum has also been demonstrated. It is expected that the ring resonator laser formed by the polymer nanowire would be a promising component in future nanophotonic devices.

■ AUTHOR INFORMATION

Corresponding Author

*E-mail: stslbj@mail.sysu.edu.cn.

Notes

The authors declare no competing financial interest.

■ ACKNOWLEDGMENTS

This work was supported by the National Natural Science Foundation of China (11274395) and the Program for Changjiang Scholars and Innovative Research Team in University (IRT13042).

■ REFERENCES

- (1) Zhao, Y. S.; Peng, A.; Fu, H.; Ma, Y.; Yao, J. *Adv. Mater.* **2008**, *20*, 1661–1665.
- (2) Clark, J.; Lanzani, G. *Nat. Photonics* **2010**, *4*, 438–446.
- (3) Yao, W.; Yan, Y.; Xue, L.; Zhang, C.; Li, G.; Zheng, Q.; Zhao, Y. S.; Jiang, H.; Yao, J. *Angew. Chem.* **2013**, *125*, 8875–8879.
- (4) Kim, F. S.; Ren, G.; Jenekhe, S. A. *Chem. Mater.* **2011**, *23*, 682–732.
- (5) Cui, Q. H.; Zhao, Y. S.; Yao, J. *Chem. Sci.* **2014**, *5*, 52–57.
- (6) O'Brien, G. A.; Quinn, A. J.; Tanner, D. A.; Redmond, G. *Adv. Mater.* **2006**, *18*, 2379–2383.
- (7) Camposeo, A.; Di Benedetto, F.; Stabile, R.; Neves, A. A.; Cingolani, R.; Pisignano, D. *Small* **2009**, *5*, 562–566.
- (8) Fasano, V.; Polini, A.; Morello, G.; Moffa, M.; Camposeo, A.; Pisignano, D. *Macromolecules* **2013**, *46*, 5935–5942.
- (9) O'Carroll, D.; Lieberwirth, I.; Redmond, G. *Nat. Nanotechnol.* **2007**, *2*, 180–184.
- (10) Noy, A.; Miller, A. E.; Klare, J. E.; Weeks, B. L.; Woods, B. W.; DeYoreo, J. J. *Nano Lett.* **2002**, *2*, 109–112.
- (11) O'Carroll, D.; Lieberwirth, I.; Redmond, G. *Small* **2007**, *3*, 1178–1183.
- (12) Yoon, S. M.; Lee, J.; Je, J. H.; Choi, H. C.; Yoon, M. *ACS Nano* **2011**, *5*, 2923–2929.
- (13) Cui, Q. H.; Zhao, Y. S.; Yao, J. *J. Mater. Chem.* **2012**, *22*, 4136–4140.
- (14) Liu, W.; Wei, J.; Chen, Y.; Huo, P.; Wei, Y. *ACS Appl. Mater. Interfaces* **2013**, *5*, 680–685.
- (15) Meng, C.; Xiao, Y.; Wang, P.; Zhang, L.; Liu, Y.; Tong, L. *Adv. Mater.* **2011**, *23*, 3770–3774.
- (16) Guo, X.; Ying, Y.; Tong, L. *Acc. Chem. Res.* **2013**, *47*, 656–666.
- (17) Song, Q.; Liu, L.; Xu, L. *J. Lightwave Technol.* **2009**, *27*, 4374–4376.
- (18) Hill, M. T.; Dorren, H. J.; De Vries, T.; Leijtens, X. J.; Den Besten, J. H.; Smalbrugge, B.; Oei, Y.-S.; Binsma, H.; Khoe, G.-D.; Smit, M. K. *Nature* **2004**, *432*, 206–209.
- (19) Xu, F.; Pruneri, V.; Finazzi, V.; Brambilla, G. *Opt. Express* **2008**, *16*, 1062–1067.
- (20) Sumetsky, M.; Dulashko, Y.; Windeler, R. *Opt. Lett.* **2010**, *35*, 1866–1868.
- (21) Li, Z.; Zhang, Y. *Angew. Chem.* **2006**, *118*, 7896–7899.
- (22) Di Stasio, F.; Grim, J. Q.; Lesnyak, V.; Rastogi, P.; Manna, L.; Moreels, I.; Krahne, R. *Small* **2014**, DOI: 10.1002/sml.201402527.
- (23) Zhang, R.; Yu, H.; Li, B. *Nanoscale* **2012**, *4*, 5856–5859.
- (24) Tong, L.; Gattass, R. R.; Ashcom, J. B.; He, S.; Lou, J.; Shen, M.; Maxwell, I.; Mazur, E. *Nature* **2003**, *426*, 816–819.
- (25) Gómez, D. E.; Pastoriza-Santos, I.; Mulvaney, P. *Small* **2005**, *1*, 238–241.
- (26) Li, H.; Li, J.; Qiang, L.; Zhang, Y.; Hao, S. *Nanoscale* **2013**, *5*, 6297–6302.
- (27) Kango, S.; Kalia, S.; Celli, A.; Njuguna, J.; Habibi, Y.; Kumar, R. *Prog. Polym. Sci.* **2013**, *38*, 1232–1261.
- (28) Enz, E.; La Ferrara, V.; Scalia, G. *ACS Nano* **2013**, *7*, 6627–6635.
- (29) Pauzauskie, P. J.; Sirbully, D. J.; Yang, P. *Phys. Rev. Lett.* **2006**, *96*, 143903.

(30) Melli, M.; Polyakov, A.; Gargas, D.; Huynh, C.; Scipioni, L.; Bao, W.; Ogletree, D.; Schuck, P.; Cabrini, S.; Weber-Bargioni, A. *Nano Lett.* **2013**, *13*, 2687–2691.

(31) Renner, J.; Worschech, L.; Forchel, A.; Mahapatra, S.; Brunner, K. *Appl. Phys. Lett.* **2006**, *89*, 231104.

(32) Lai, C.-M.; Wu, H.-M.; Huang, P.-C.; Wang, S.-L.; Peng, L.-H. *Appl. Phys. Lett.* **2007**, *90*, 141106.